molecular pharmaceutics

Article

pubs.acs.org/molecularpharmaceutics

Lactoferrin-Modified Poly(ethylene glycol)-Grafted BSA Nanoparticles as a Dual-Targeting Carrier for Treating Brain Gliomas

Zhigui Su,† Lei Xing,† Yinan Chen,† Yurui Xu, Feifei Yang, Can Zhang, Qineng Ping, and Yanyu Xiao*

Department of Pharmaceutics, State Key Laboratory of Natural Medicines, China Pharmaceutical University, Nanjing 210009, P. R. China

ABSTRACT: In this study, a dual-targeting drug delivery system based on bovine serum albumin nanoparticles (BSA-NPs) modified with both lactoferrin (Lf) and mPEG2000 loading doxorubicin (DOX) was designed, and its blood−brain barrier (BBB) penetration and brain glioma cells targeting properties were explored. BSA-NPs were prepared by a desolvation technique, and mPEG2000 was incorporated onto the surface of BSA-NPs by reacting with the free amino-group of BSA to form mPEG2000-modified BSA-NPs (P_{2000}-NPs). Finally, Lf-modified P_{2000}-NPs (Lf-NPs) was obtained by absorbing Lf onto the surface of P_{2000}-NPs via the positive and negative charges interaction at physiological pH. Three levels of mPEG2000 and Lf-modified NPs were prepared and characterized, respectively. The uptake and potential cytotoxicity of different DOX preparations in vitro by the primary brain capillary endothelial cells (BCECs) and glioma cells (C6) were investigated. The dual-targeting effects were studied on the BBB model in vitro, BCECs/C6 glioma coculture model in vitro, and C6 glioma-bearing rats in vivo, respectively. The results exhibited that, with the increase of the amount of both mPEG2000 and Lf, the particle size of NPs increased and its zeta potential decreased. The in vivo pharmacokinetics study in healthy rats exhibited that P_{2000}-NPs with a high level of mPEG2000 (P_{2000H}-NPs) had longer circulation time in vivo. Compared to other NPs, Lf-NPs with high level of both Lf and mPEG2000 (Lf_H-NPs) showed the strongest cytotoxicity and the highest effectiveness in the uptake both in BCECs and C6 as well as improved the dual-targeting effects. Body distribution of DOX in different formulations revealed that Lf_H-NPs could significantly increase the accumulation of DOX in the brain, especially at 2 h postinjection ($P < 0.05$). In conclusion, Lf-NPs were a prospective dual-targeting drug delivery system for effective targeting therapy of brain gliomas.

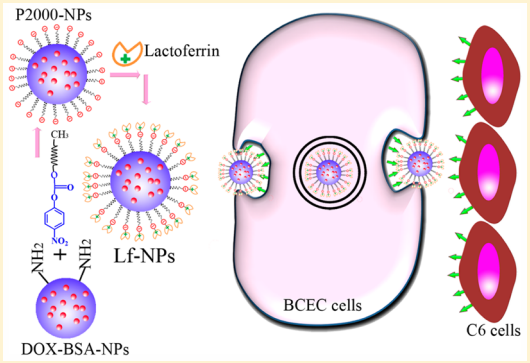

KEYWORDS: *dual-targeting, lactoferrin, mPEG2000, bovine serum albumin nanoparticles, electrostatic interaction, gliomas*

INTRODUCTION

Gliomas, as an intracranial malignant tumor, are responsible for almost 40% of all brain tumors.[1] On the basis of the location and degree of lesion, lots of strategies are applied for treating gliomas including surgery, radiation therapy, and chemotherapy.[2] Being the most common initial treatment for gliomas, surgery of course could remove most of the tumor directly from the brain. However, because of the infiltration into normal surrounding brain parenchyma, remaining tumor cells would lead to inevitable relapse of glioma. Radiation therapy usually follows surgery to destruct tumor cells locating where the surgery is not safe. The dose of radiation need to be high enough to be effective, but it is difficult for the normal tissue to be tolerant under such a high dose.[3] Therefore, chemotherapy, especially targeted therapy, is recommended after surgery and radiation therapy.

However, because of the main obstacle of the blood−brain barrier (BBB), common chemotherapeutics cannot reach the location of brain tumor such as gliomas.[4] Meanwhile, because of its no-specific targeting ability, it is also difficult to differentiate the tumor site with normal tissues for therapeutic agents. As a result, developing a drug delivery system (DDS) that penetrates BBB and targets to gliomas has already drawn attention. Compared with other strategies, nanocarriers modified with targeting moieties are researched lying on several advantages, such as increased stability of drug, favorable pharmacokinetics, enhanced delivery of drug to brain, etc. Moreover, dual targets to both BBB and gliomas allow the pharmaceutical index to be optimized. When doxorubicin (DOX)-loaded liposomes were conjugated with *p*-aminophenyl-α-D-mannopyranoside (MAN) and transferring (Tf), the transport ratio across the BBB model was significantly increased from 3.11% to 24.9%, and the inhibitory rate to C6 cells after crossing the BBB increased from 45.5% to 64.0% when compared to free DOX.[5] He et al. developed a dendrimer-based drug delivery carrier based on polyether-copolyester structure and two targeting moieties: transferrin (Tf) and wheat germ agglutinin (WGA). The results demonstrated that Tf could enhance the transport of the

Received: November 7, 2013
Revised: April 22, 2014
Accepted: April 29, 2014
Published: April 29, 2014

dx.doi.org/10.1021/mp500238m | *Mol. Pharmaceutics* 2014, 11, 1823−1834

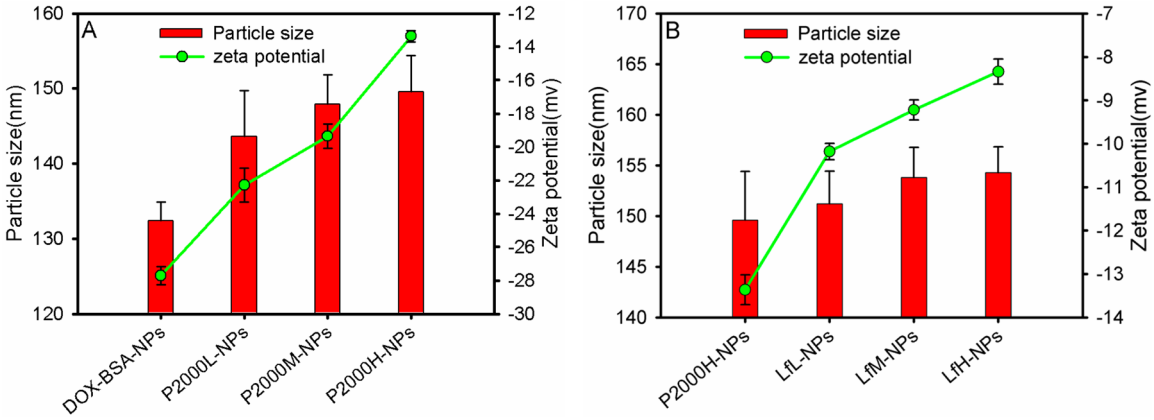

Figure 1. Particle size and zeta potential of nanoparticles: (A) P_{2000}-NPs and (B) Lf-NPs. Data were presented as the mean ± SD (n = 3).

BBB and ascribe to the targeting effect of Tf and WGA that this carrier completely broke the avascular C6 spheroids in vitro.[6] As is known to all, to synthesize such targeted-ligand-based carriers many factors would affect the targeting efficiency in vivo.[7] A dual-targeting carrier with only one targeted ligand applied to treat gliomas can overcome the shortcomings of multitargeted-ligand-based carriers because some receptors are existing not only on BBB in different species but also on the cell surface of glioblastomas, such as Tf receptor and low density lipoprotein receptor.[8] Pang et al. used biodegradable polymersomes linking with Tf (TF-PO) as glioma targeting system. The brain tumor distribution showed that compared to free DOX, the average concentration of DOX in gliomas increased 7.1-folds for Tf-PO−DOX.[9] However, a simple way to coujugate a ligand to the carrier is considerable to avoid the loss of a target's activity during chemical synthesis. Lactoferrin (Lf), an iron binding glycoprotein with relative molecular weight 80 kDa, can mediate drug delivery system to transport across BBB.[10] What is more, low-density lipoprotein receptor-related protein (LRP), the receptor of Lf, was proved overpressed in glioma cells so that Lf could mediate the transcytosis of carriers into glioma cells.[11] Hence, Lf can be served as a BBB and glioma dual targeting ligand, which enhanced the penetrating ability to overcome BBB and realized specific glioma targets. Moreover, with positive charge at physiological pH,[12] Lf could easily absorb onto the surface of negative nanocarriers via electrostatic interaction, which would be beneficial to preserve the biological activity of Lf without chemical conjugation process.

As known to all, protein-based nanoparticles possess several advantages including greater stability during storage and in vivo, being nontoxic and nonantigenic and easy to scale up during manufacture.[13] As a biodegradable and nonimmunogenic material, albumin can be utilized as functional material for constructing macromolecular carrier and nanoparticle preparation.[14] With negative charge at physiological pH of albumin-based nanoparticles, positive charged molecules (e.g., Lf) could adsorb onto the surface via electrostatic interaction. In addition, albumin based nanoparticles could be easily prepared under moderate conditions by coacervation, controlled desolvation, or emulsion formation to load and maintain the activity of drugs.[15] In our preliminary studies, the DOX-loaded bovine serum albumin nanoparticles (DOX-BSA-NPs) had been prepared. Pharmacokinetic study in rats showed that after intravenous administration of DOX-BSA-NPs the concentration of DOX in plasma decreased rapidly. To solve this problem, modification of PEG to proteins or particles is an effective strategy to prolong their circulation in vivo, reduce their immunogenicity, and enhance their accumulation in tumors by enhanced permeability and retention (EPR) effect.[16]

On the basis of the above considerations, it is the first report on using terminal group activated mPEG2000 to construct PEGylated BSA-NPs (P_{2000}-NPs) as the carrier loading DOX as a model antitumor drug. Then with the help of electrostatic interaction, Lf, with positive charge at physiological pH, could absorb onto the surface of P_{2000}-NPs to construct a dual-targeting brain drug delivery system (Lf-NPs) to overcome BBB and target gliomas (Figure 1). In the present study, three levels of mPEG2000 and Lf-modified NPs were prepared and characterized, respectively, and the average density of Lf and mPEG2000 on the surface of Lf-NPs was quantified. The uptake and potential cytotoxicity of various DOX formulations in vitro by the primary brain capillary endothelial cells (BCECs) and glioma cells (C6) were evaluated. The dual-targeting effects were investigated on the BBB model in vitro, BCECs/C6 glioma coculture model in vitro, and C6 glioma-bearing rats in vivo, respectively. In vivo pharmacokinetics in healthy rats were studied. Finally, distribution of DOX after intravenous administration of different DOX formulations to glioma model rats was used to evaluate their target-glioma activity.

MATERIALS AND METHODS

Materials and Animals. Bovine serum albumin (BSA, purity 98%) was purchased from Shanghai Yiming Biotechnology Co. Ltd. (Shanghai, China). Doxorubicin hydrochloride (DOX·HCl, purity 99.2%) was purchased from RPG Life Sciences Company (India). Pepsin from porcine gastric mucosa, poly(ethylene glycol) methyl ether 2000 (mPEG2000, M_n 2000), lactoferrin (human, ≥ 90% SDS-PAGE), and 3-(4,5-dimethylthiazol-2-yl)-2,5-diphenyltetrazolium bromide (MTT) were from Sigma-Aldrich (Milwaukee, WI, USA). 4-Nitrophenyl chloroformate (pNP) was from Suzhou Time-Chem Technologies Co. Ltd. (Suzhou, China). Glutaraldehyde (25% solution), iodine, and potassium iodide were from Sinopharm Chemical Reagent Co. Ltd. (Shanghai, China). All other chemicals and reagents were of analytical grade and used without further purification.

Sprague−Dawley rats (weighing 180−220 g) were purchased from Experiment Animal Centre of Nantong University (Nantong, China). The animals involved in this study were treated according to protocols evaluated and approved by the ethical committee of China Pharmaceutical University.

Cell Culture. In this study, rat brain capillary endothelial cells (BCECs) and glioma cells (C6) were used. BCECs were kindly provided by Prof. Zhang (Department of Pharmacology, China Pharmaceutical University) and cultured in the endothelial cell culture medium that contained DMEM/F12, 20% heated-inactivated fetal bovine serum (FBS), 100 U/mL penicillin, and 100 μg/mL streptomycin. C6 glioma cells were kindly provided by Prof. Guo (Department of Pharmacology, China Pharmaceutical University) and routinely grown in DMEM medium supplemented by 10% FBS, 100 U/mL penicillin, and 100 μg/mL streptomycin. Cells were maintained at 37 °C in the presence of 5% CO_2.

Synthesis of pNP-mPEG2000. 4-Nitrophenyl chloroformate-mPEG2000 (pNP-mPEG2000) was synthesized as described previously in our laboratory[17] with subtle modification. Briefly, 5 g of mPEG2000 was dissolved in 18 mL of dichloromethane and then was supplemented with 0.42 mL of triethylamine (TEA). Then, 0.71 g of 4-nitrophenyl chloroformate dissolved in 2 mL of dichloromethane was added to the mixture, and the sample was incubated overnight at room temperature under the constant stirring. Then, the organic solvents were removed using a rotary evaporator, and the residues were recrystallized and purified to obtain pNP-mPEG2000.[17,18] The structure of pNP-mPEG2000 was characterized by TLC and ^{1}H NMR spectrum (AVANCE AV-300, Bruker Instrument Inc., Switzerland) using $CDCl_3$ as a solvent at 25 °C.

Preparation and Charaterization of Different DOX-Loaded-NPs. DOX-loaded Lf-NPs were prepared as follows. First, DOX-BSA-NPs were prepared by a desolvation technique as described previously with slight modification.[19] Briefly, BSA (20 mg) and DOX (1 mg) were dissolved in 2 mL of deionized water with pH 8.0 (adjusted with 0.1 M NaOH). Under constant stirring (600 rpm) at room temperature, 7 mL of ethanol were added dropwisely at the rate of 0.1 mL/min using a constant flow pump. Then, 2.5% glutaraldehyde solution (1 μL/mg BSA) was added into DOX-BSA-NPs. The cross-linking process was done with continuous stirring for 24 h to obtain stable DOX-BSA-NPs.[20] After reaction, the ethanol was removed using rotary evaporation. The resulting DOX-BSA-NPs were purified by centrifugation (18 000 rpm, 30 min, HITACHI, Japan) and redispersed in purified water for three times to remove extra glutaraldehyde. Next, mPEG2000-modified DOX-BSA-NPs (P_{2000}-NPs) were prepared by reacting DOX-BSA-NPs with pNP-mPEG2000.[18] Briefly, 20, 100, or 300 μL of pNP-mPEG2000 with concentration of 65 mg/mL was added into 20 mg/mL nanoparticles in 0.1 M sodium bicarbonate buffer (pH 8.5). After constant stirring (600 rpm) for 2 h, the nanoparticles were purified by centrifugation (18 000 rpm, 60 min), washed with purified water for three times, and redispersed with purified water. Low, medium, and high levels of mPEG2000-modified DOX-BSA-NPs were coded as P_{2000L}-NPs, P_{2000M}-NPs, and P_{2000H}-NPs, respectively. Finally, Lf-modified P_{2000H}-NPs (Lf-NPs) were prepared by incubating P_{2000H}-NPs with Lf solution. Briefly, 1, 2, or 2.5 mg/mL of Lf solution dissolved in Tris-EDTA buffer (pH 7.4) was gently mixed with an equal volume of P_{2000H}-NPs, respectively. The mixture was incubated for 24 h at 4 °C. Then Lf-NPs were purified by centrifugation (18 000 rpm, 60 min) to remove free Lf, washed with purified water for three times, and redispersed with purified water. Following the same procedure, three levels of Lf-modified P_{2000H}-NPs was prepared, named as Lf_L-NPs, Lf_M-NP, and Lf_H-NPs, respectively.

The particle size, polydispersity index (PI), and zeta potential of the preparations (BSA-NPs, P_{2000}-NPs, and Lf-NPs) were detected by Zeta Plus (Brookehaven, USA). Drug loading capacity (DLC) and entrapment efficiency (EE) of DOX and yield of BSA-NPs were determined as previously reported.[21]

Surface mPEG Densities of P_{2000}-NPs and Surface Lf Densities of Lf-NPs. The suspension of P_{2000}-NPs was centrifugated (18 000 rpm, 60 min), and the supernatant (i.e., unreacted pNP-mPEG2000, defined as W_1) was determined by colorimetric method.[22] Then, the concentration of mPEG2000 was calculated from a standard curve in a range from 0.5 to 7.5 μg mPEG/mL. The amount of total mPEG in the suspension of P_{2000}-NPs (including the unreacted and reacted pNP-mPEG), defined as W_2, were directly measured without centrifugation. The amounts of mPEG reacted on the surface of P_{2000}-NPs (W_{mPEG}) were equal to (W_2−W_1). The surface density of mPEG chains (SD_{PEG}) could be worked out via dividing the total number of mPEG chains (N_{PEG}) by the nanoparticle surface area (S_{NP}):[22]

$$SD_{mPEG} = N_{mPEG}/S_{NP}$$

Resolving, $N_{mPEG} = (W_{mPEG}/MW_{mPEG}) \times A_n$, where W_{mPEG} is equal to ($W_2 - W_1$), MW_{mPEG} is the molecular weight of mPEG, and A_n is Avogadro's number. $S_{np} = 4\pi r^2 N_{BSA\text{-}NP}$, $N_{BSA\text{-}NP}$ is the total number of nanoparticles and r is approximate to the whole particle radius. The distance between PEG chains on the surface of P_{2000}-NPs (D_{PEG}) was calculated as follows:

$$D_{PEG} = \sqrt{1/SD_{mPEG}}$$

The modification efficiency (ME) of mPEG was calculated as follows:

$$ME_{mPEG}(\%) = N_{mPEG}/N_{-NH_2} \times 100\%$$

where N_{-NH2} is the free amino group on the surface of BSA-NPs and determined by colorimetric method.[23]

The amounts of nonadsorbed Lf molecules, defined as W_3, were obtained by centrifugation (18 000 rpm, 60 min) and determined with Coomassie Brilliant Blue and calculated using Lf reference standard. The amounts of total Lf molecules (including the nonadsorbed and adsorbed Lf molecules), defined as W_4, were obtained like this: Lf was dissolved in Tris-EDTA buffer (pH 7.4) and added into equal volume of purified water without P_{2000H}-NPs and directly measured without centrifugation. Thus, the amounts of Lf molecules adsorbed on the surface of Lf-NPs were equal to ($W_4 - W_3$). The ME of Lf molecule was calculated as follows:

$$ME_{Lf}(\%) = (W_4 - W_3)/W_4 \times 100\%$$

The number of Lf per P_{2000H}-NPs was calculated as follows:

$$N = N_{Lf}/N_{P2000H\text{-}NPs}$$

Resolving, $N_{Lf} = (W_{Lf}/MW_{Lf}) \times A_n$, where W_{Lf} is equal to ($W_4 - W_3$), MW_{Lf} is the molecular weight of Lf, and A_n is Avogadro's number. $N_{P2000H\text{-}NPs}$ is the total number of P_{2000H}-NPs.

In Vitro Release Study of Different DOX-Loaded-NPs. The experiment of DOX released from NPs was performed in saline using a membrane dialysis apparatus. One milliliter of different preparations of DOX (containing 200 μg of DOX) and 1 mL of saline were placed into a preswelled dialysis bag (8−10 kDa MW cutoff, Sigma, USA). DOX solution was served

as control. The bag was tightened and soaked in 50 mL of saline. The release process remains in sink conditions at 37 °C for 48 h (n = 3). At a given time interval, 5 mL of the medium was withdrawn and replaced with the same amount of prewarmed fresh medium. The concentration of DOX in the medium was determined using a spectrophotometer (wavelength at 480 nm). To imitate the microenvironment in plasma, saline containing 20 μg/mL of trypsin was used as release medium instead of saline alone.[24] The other procedure was the same as above.

In Vitro Cytotoxicity of Different DOX-Loaded-NPs against BCECs and C6. Cells viabilities were determined by MTT assay. Briefly, for BCECs, 5×10^3 cells/well were seeded in 96-well culture plates and grown for 24 h. Then cells were cocultured with free DOX, blank BSA-NPs, blank P_{2000H}-NPs, blank Lf-NPs, and different DOX-loaded-NP, respectively. The concentration of blank carrier was in the range of 2−200 μg/mL and the final concentration of DOX was in the range of 0−8 μg/mL. After 24 h incubation, 10 μL of 5 mg/mL MTT were added into each well for 4 h in dark, and then, the medium was then replaced with 150 μL of DMSO. The absorbance value at 570 nm (A_{570nm}) was read using the microplate reader (Thermo Electron Corporation. USA). Cell viability was expressed as a percentage of A_{570nm} of the study group relative to that of control group. The cytotoxicity study against C6 was conducted in the same process.

In Vitro BBB Model and BBB Transport Experiment. To investigate BBB transportation of different DOX-loaded nanoparticles, BCECs was applied to constructed the BBB monolayer model.[25] BCECs (7.5×10^4 cells/well) were seeded onto 2% gelatin pretreated polycarbonate membrane transwell inserts (0.4 μm mean pore size, 12 mm diameter, and 0.6 cm^2 surface areas, Millicpore, Carrigtohill, Co. Cork, Ireland) and cultured for 10 days at 37 °C. The culture medium was changed every 2 days. To confirm the integrality of BBB, the transendothelial electrical resistance (TEER) of monolayer model was determined by a TEER instrument (Word Precision Instruments, Inc. Sarasota, FL, USA). Only the plates with TEER value over 250 Ω cm^2 were selected as the BBB model.[26,27]

The BBB transport experiment was preceded as follows:[28] free Dox, BSA-NPs, P_{2000H}-NP, and Lf_H-NP were added into the donor compartment of BBB model with the DOX concentration of 5 μg/mL at 37 °C. For the competition assay, 0.1 mg/mL of Lf were pretreated with BBB model for 30 min, and then Lf_H-NP was added with final DOX concentration at 5 μg/mL. At 30, 60, 90, and 120 min, 150 μL medium was withdrawn from acceptor compartments for each well and then replaced 150 μL of fresh medium immediately. The concentration of DOX in acceptor medium was determined using HPLC with fluorescence detector and the excitation and emission wavelengths were 480 and 550 nm, respectively. The apparent permeability coefficient (P_e) was obtained from the slope of accumulated concentration versus time curve equation:[29]

$$P_e = (dQ/dt) \times (1/AC_0)$$

where dQ is the amount of DOX in the basolateral side at time t, A is the diffusion area, and C_0 is the initial concentration of DOX in the apical side.

In Vitro Cellular Uptake Assay in BCECs and C6 Cells and Study on the Uptake Mechanism by C6 Glioma Cells. Five × 10^5 cells/well of BCECs and C6 were seeded into 6-well culture plates and incubated at 37 °C for 24 h. Free DOX, BSA-NPs, P_{2000H}-NPs, Lf_L-NPs, Lf_M-NPs, and Lf_H-NPs were added to the cells at 5 μg/mL of DOX, respectively, cells were incubated for another 2 h. To reveal the possible uptake mechanism by C6, the following inhibitors were applied to preincubate with C6 at 37 °C for 30 min: (1) Lf (0−100 μg/mL); (2) sodium azide (0.1%, w/v), a cell energy metabolism inhibitor;[30] (3) NH_4Cl (10 mM), a cell endosome/lysosome formation inhibitor;[31] (4) mannitol (200 mM), inhibitor of clathrin-mediated endocytosis;[32] (5) nystatin (15 μg/mL), inhibitor of caveolin-mediated endocytosis;[33] and (6) amiloride (5 mM), inhibitor of macropinocytosis;[34] then DOX-loaded NPs at a concentration of 5 μg/mL were added and incubated at 37 °C for an additional 4 h. Cells without pretreating any inhibitor were used as a blank control. After incubation, cells were washed three times with pH 7.4 PBS at 4 °C, and the cells were lysed with 0.4 mL of 1% Triton X-100 for 3 min. Twenty microliters of the cell lysate from each well was used to determine the total cell protein content via the BCA protein assay kit. The concentration of DOX in cell lysate was determined using HPLC method (Agilent 1200). The uptake index (UI) was expressed as DOX (μg)/protein (mg). The relative uptake index (R_{UI}) was

$$R_{UI} = UI_S/UI_C \times 100\%$$

where UI_S is the UI of DOX-loaded NPs treated with various kinds of uptake inhibitors and UI_C is the UI of controls.

In Vitro Dual-Targeting Effects. To establish the BCECs/C6 coculture model, BBB model established as described above was inserted into the 12-well plates in which were precoated with C6 cells for 48 h. After adding 400 μL of free DOX, DOX-BSA-NPs, P_{2000H}-NPs, and Lf_H-NPs at the concentration of 5 μg/mL of DOX into the donor compartment 2 h later, respectively, the insets were removed and C6 was allowed to culture for another 12 h. The amount of DOX uptaken by C6 was determined by the HPLC as reported above.

Pharmacokinetics Studies in Rats. Healthy SD rats were used to evaluate the effect of the amount of mPEG2000 and Lf on pharmacokinetics of DOX. The concentration of DOX in plasma was measured via HPLC with fluorescence detector, and the excitation and emission wavelengths were 480 and 550 nm, respectively. After blood collection, the plasma was obtained by centrifugation at 4000 rpm for 10 min and frozen at −20 °C until assay. Then, 150 μL of 10% pepsin solution was added into 100 μL of plasma and vortexed for 2 min and then incubated for 20 min at 37 °C. After incubation, 200 μL of ethyl acetate/methanol (1:1, v/v) was added into the above mixture, vortexed for 2 min, and centrifuged at 12 000 rpm for 10 min. To determine the concentration of DOX, 20 μL of supernatant was injected into the HPLC system. Different preparations at a dose of 5 mg/kg were injected into the tail vein of rats (n = 6), and at predetermined intervals the blood samples were collected. The DOX concentration in plasma was analyzed by Kinetica 4.4.

Bistribution in Glioma Model Rats. To establish the gliomas model, C6 was stereotactically injected into the right striatum of outbred Wistar rat and then the rats were raised for 10 days to grow tumor in brain. After intravenous administration of BSA-NPs, P_{2000H}-NPs, or Lf_H-NPs at a dose of 5 mg/kg, the rats were sacrificed by cervical dislocation at the time intervals of 10, 30, and 120 min, respectively. Blood samples and the major tissues were collected, and all tissues samples were washed by physiological saline, then weighed and

stored at −20 °C until analyzed. DOX solution was used as control. Frozen tissues were thawed and homogenized with physiological saline (1.5 mL/g tissue) using a tissue homogenizer. The concentrations of DOX in plasma and homogenates of tissues were determined as described above.

Statistical Data Analysis. Results are given as mean ± SD. Statistical significance was tested by two-tailed Student's *t* test or one-way ANOVA. Statistical significance was set at $P < 0.05$.

RESULTS AND DISCUSSION

Preparation and Characterization of DOX-Loaded-NPs. The desolvation method was chosen to prepare DOX-BSA-NPs because of the simple operation and more importantly controllable degree of cross-linking according to the amount of glutaraldehyde and setting time. The volume of ethanol was 3.5 times that of DOX/BSA solution so that the EE and yield of DOX-BSA-NPs were 98.5 ± 3.9% and 96.5 ± 1.2%, respectively. DLC of DOX in DOX-BSA-NPs was 4.3 ± 0.1%. The amount of glutaraldehyde could cross-link about 50% of amino groups of total BSA theoretically to make sure there were enough free amino groups for further modification.[35]

The particle size, PI, and zeta potential of different formulations are shown in Figure 1. The modification of mPEG2000 or Lf resulted in the increase of the particle size compared with DOX-BSA-NPs or P_{2000H}-NPs. The increase of particle size might be caused through different mechanisms. For P_{2000}-NPs, the increase of particle size might be owned to graft the PEG chains onto the surface of DOX-BSA-NPs by amide bond; however, the increase of fixed aqueous layer thickness (FALT) might also attribute to the increase of particle size.[36] However, electrostatic interaction between negatively charged and positively charged Lf surface of P_{2000H}-NPs resulted in the formation of Lf-NPs. The more the Lf was used, the larger the particle size. As reported previously, with 100−200 nm diameter nanoparticles would prolong the circulation in blood due to avoid phagocytosis by RES and accumulate in tumors by ERP.[37]

As shown in Figure 1A, the increase of mPEG2000 on the surface of DOX-BSA-NPs would mask the negative charge, which lead to the increase of zeta potential.[38] The more the mPEG2000, the less the absolute value of zeta potential. In addition, in Figure 1B, as the amounts of Lf increased, the negative zeta potential of P_{2000H}-NPs was further neutralized by electrostatic interaction. Moreover, the threshold of zeta potential for agglomeration in dispersion was about −20 mV;[39] thus, the absolute value of zeta potential for P_{2000}-NPs or Lf-NPs presented here was too low to obtain sufficient electrostatic stabilization. However, both mPEG2000 and Lf were hydrophilic and could provide additional steric stabilization for modified BSA-NPs.[30]

Average Density of mPEG on the Surface of P_{2000}-NPs and Lf Molecules on the Surface of Lf-NPs. From Table 1, SD_{PEG} of P_{2000H}-NPs was 6.81-fold and 1.47-fold higher than that of P_{2000L}-NPs and P_{2000M}-NPs, respectively, which was corresponding with the value of ME_{mPEG}. A previous study demonstrated that SD_{mPEG} was affected by the modification level of PEG, the molecular weight of hydrophilic chains, and particle size.[40] The greater increase in the amount of PEG used, the higher SD_{PEG}.

Table 1. ME_{mPEG}, SD_{mPEG}, and D_{PEG} (nm) of P_{2000}-NPs; Data Were Presented as the Mean ± SD (n = 3)

preparations	ME_{mPEG} (%)	SD_{mPEG}	D_{PEG} (nm)
P_{2000L}-NPs	16.92 ± 0.42	0.032 ± 0.001	5.59 ± 0.09
P_{2000M}-NPs	76.54 ± 1.44	0.148 ± 0.002	2.60 ± 0.02
P_{2000H}-NPs	111.69 ± 1.08	0.218 ± 0.002	2.14 ± 0.01

In addition, D_{PEG} of P_{2000L}-NPs and P_{2000M}-NPs was 2.61-fold and 1.21-fold wider than that of P_{2000H}-NPs, respectively. With the increase of $ME_{mPEG2000}$ from 16.92% to 111.69%, D_{PEG} decreased, suggesting that two neighboring PEG grafting sites got narrow. If D_{PEG} was less than the radius of most of the plasma proteins (2−5 nm), the absorption of protein and phagocytosis of RES would be hindered,[41] but longer circulation time in vivo would be achieved. Hence, it is not enough to prevent the adsorption of proteins at low level of modification of PEG (16.92%). While the amounts of mPEG2000 reached at medium and high levels of modification (76.54 and 111.69%) D_{PEG} decreased to 2.60 and 2.14 nm, this indicated that long circulation in vivo of P2000-NPs might be achieved at these two levels of modification.

It was well-known that Lf receptor distributed over the cell membrane and presented clusters are featured.[42] If receptor-mediated transport was the predominant process for the cellular uptake of nanocarriers, higher cellular uptake might occur with appropriate density of ligand molecules on the surface of nanocarriers. In this study, three levels of Lf were used to modify P_{2000H}-NPs (Table 2). With the amounts of Lf used increased, more Lf were absorbed on the surface of P_{2000H}-NPs, which was in consistent with the decrease of absolute value of zeta potential in Figure 1B.

Table 2. ME_{Lf} and Number of Lf per Lf-NPs; Data Were Presented as the Mean ± SD (n = 3)

preparations	Lf (mg/mL)	ME_{Lf} (%)	N (number)
Lf_L-NPs	1	98.00 ± 3.26	2584 ± 158
Lf_M-NPs	2	84.59 ± 5.50	4483 ± 580
Lf_H-NPs	2.5	94.86 ± 7.63	6276 ± 1002

In Vitro Release Study of DOX-Loaded NPs. In Figure 2 except for DOX solution, all preparations exhibited a sustained release of DOX, which could be attributed to the protection of DOX encapsulated into NPs. Comparing Figure 2A,B as well as Figure 2C,D, the presence of trypsin accelerated the release of DOX. The faster release of DOX might be ascribed to the degradation of DOX-BSA-NPs by trypsin, which increased the passive diffusion of DOX from the interior of DOX-BSA-NPs. Moreover, DOX released from P_{2000}-NPs was slower than that from DOX-BSA-NPs, and the increase of amounts of PEG applied improved sustained release effect, especially for P_{2000H}-NPs. As described above, modification of mPEG would abate the interaction of trypsin with the surface of nanoparticles, which would retard the degradation of BSA-NPs. Therefore, in the later experiments, P_{2000H}-NPs were chosen for a further study. In Figure 2C,D after modifying Lf on the surface of P_{2000H}-NPs by electrostatic interaction, the release of DOX decreased significantly ($P < 0.05$). However, modification of Lf did not affect the release of DOX from nanoparticles.

To explore the release mechanisms of DOX from DOX-loaded NPs, the zero-, first-, Higuchi release, Weibull, and reciprocal powered time (RPT) models were utilized to simulate the release profiles,[43] while Akaike discriminatory criterion value (AIC) was used to evaluate the degree of fitting of these models.[44] According to AIC, the release of DOX from

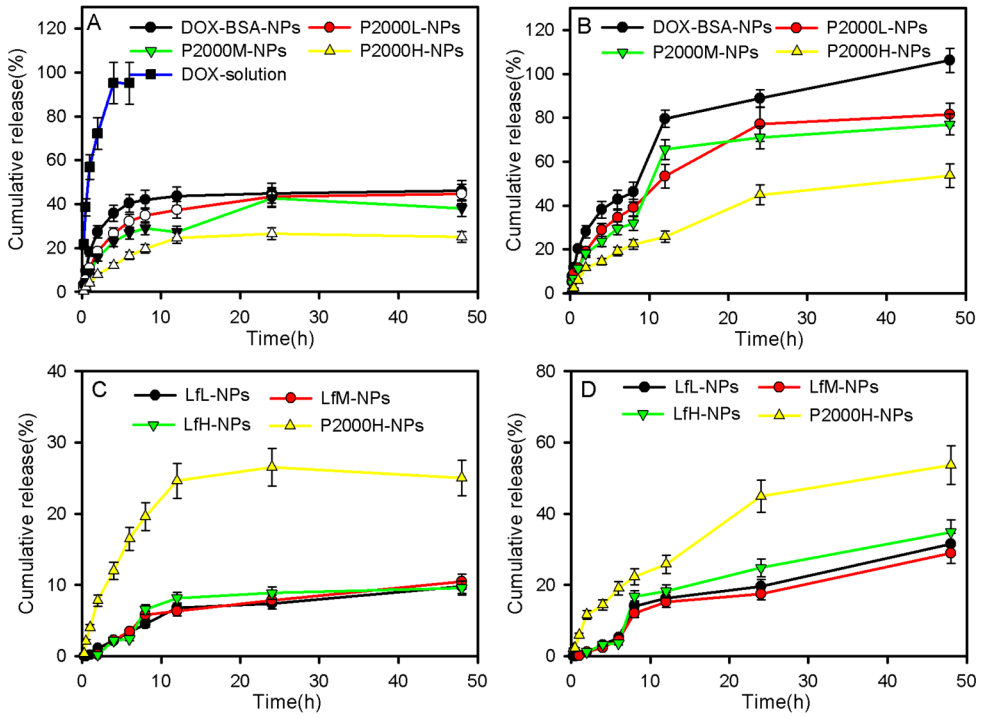

Figure 2. In vitro release curve of DOX from DOX solution and DOX-loaded NPs: (A,C) in saline and (B,D) in saline with trypsin. Data were presented as the mean ± SD (n = 3).

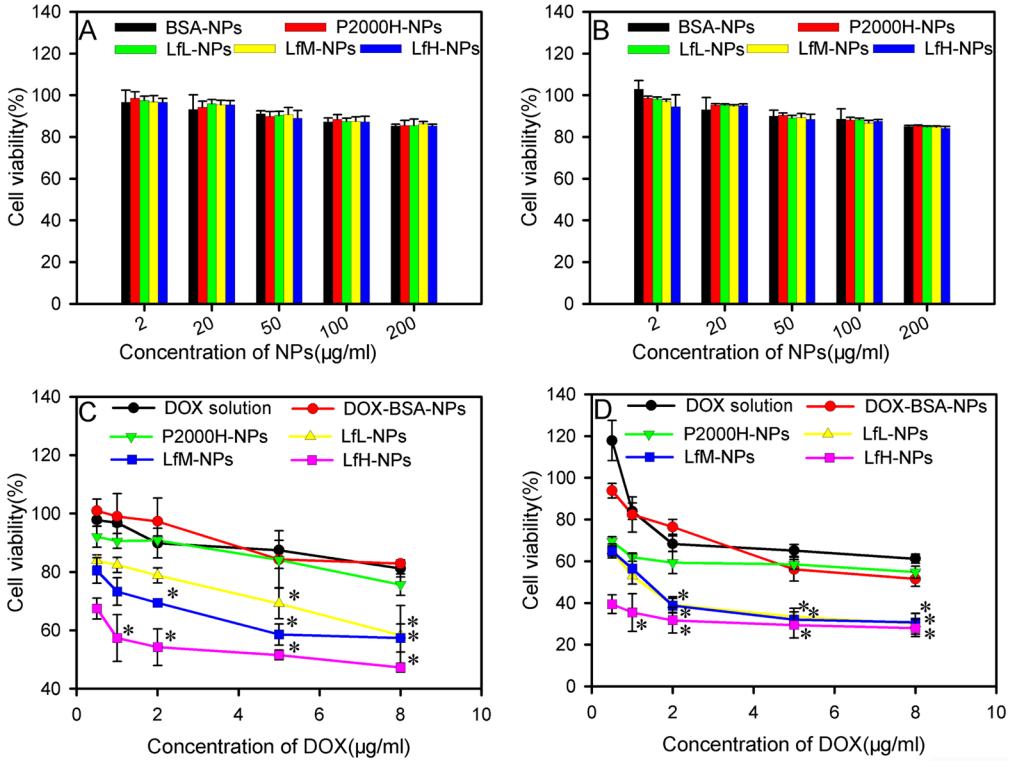

Figure 3. MTT results of different kinds of DOX-loaded preparations: (A,C) BCECs and (B,D) C6. *P < 0.05 compared with DOX solution.

DOX-loaded NPs were better fitting with Weibull and RPT models, which meant that the release mechanisms would include dissolution, diffusion, mixed dissolution diffusion, and erosion.[45]

In Vitro Cytotoxicity Assay against BCECs and C6. No significant toxicity was found for blank unmodified and modified BSA-NPs to both BCECs and C6 and even at the highest concentration of 200 μg/mL of NPs, the cell viability was more than 90% after 24 h incubation (Figure 3A,B). However, free DOX and unmodified and modified BSA-NPs loaded with DOX showed different tendency. In both BCECs and C6 cells the toxicity order was Lf_H-NPs > Lf_M-NPs > Lf_L-

dx.doi.org/10.1021/mp500238m | Mol. Pharmaceutics 2014, 11, 1823−1834

Table 3. P_e of DOX Solution, DOX-BSA-NPs, P_{2000H}-NPs, Lf_L-NPs, Lf_M-NPs, and Lf_H-NPs in BBB Model; Data Were Presented as the Mean ± SD (n = 3)

preparations	DOX solution	DOX-BSA-NPs	P_{2000H}-NPs	Lf_L-NPs	Lf_M-NPs	Lf_H-NPs
P_e (cm/h)	0.013 ± 0.002	0.008 ± 0.003	0.013 ± 0.002	0.014 ± 0.001	0.018 ± 0.003	0.074 ± 0.012
Pe ratio of NPs to DOX solution		0.62 ± 0.12	1 ± 0.24	1.08 ± 0.11	1.38 ± 0.31	5.69 ± 0.54

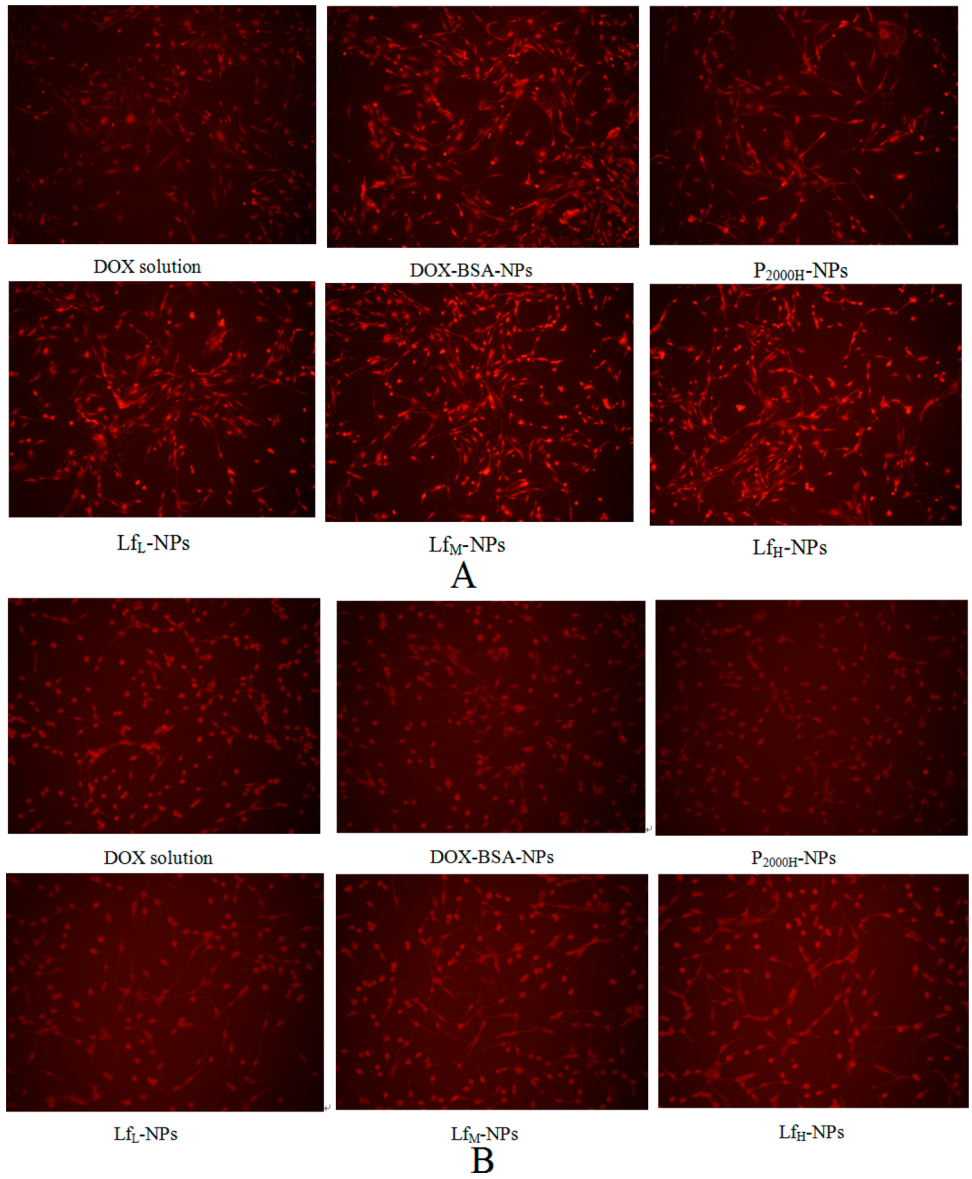

Figure 4. Fluorescent microscopy images of cells incubating with DOX solution, DOX-BSA-NPs, P_{2000H}-NPs, Lf_L-NPs, Lf_M-NPs, and Lf_H-NPs in BCECs (A) and C6 (B) at 37 °C for 2 h, respectively.

NPs > P_{2000H}-NPs ≈ DOX-BSA-NPs ≈ free DOX (Figure 3C,D). However, all of the DOX-loaded preparations exhibited higher viability against BCECs compared to C6. As candidates for CNS chemotherapy, DOX is effective in glioblastoma but lacks the ability to cross the BBB.[46] After loaded into BSA-NPs and internalized into cells by endocytosis, DOX revealed enhanced cytotoxicity in C6. Besides, the cytotoxicity assay also corresponded with the previous uptake profile (data no shown). All the results indicated that modification of Lf could improve the cytotoxicity of DOX effectively.

In Vitro BBB Model and BBB Transport Experiment. Table 3 showed the P_e of different preparations. Compared to DOX solution, the P_e of DOX-BSA-NPs decreased from 0.013 to 0.008 cm/h. The P_e of P_{2000H}-NPs improved when compared with DOX-BSA-NPs. As shown in Table 1 DOX-BSA-NPs possessed the highest negative zeta potential, and the electronic repulsion between the negative charge of DOX-BSA-NPs and C6 cells resulted in fewer DOX-BSA-NPs being adsorbed to the cell membrane.[47] Besides, appropriate hydrophilicity and lipophilicity on the surface of nanocarriers would also play an important role for the uptake by cancer cells.[48] When modified with mPEG2000, the hydrophilicity of DOX-BSA-NPs increased, which might influence the permeation effect. A slight increase of P_e value was observed when DOX loaded into low and medium level of Lf-modified NPs (1.08-fold and 1.38-fold vs free DOX, respectively), suggesting few ligand

dx.doi.org/10.1021/mp500238m | Mol. Pharmaceutics 2014, 11, 1823−1834

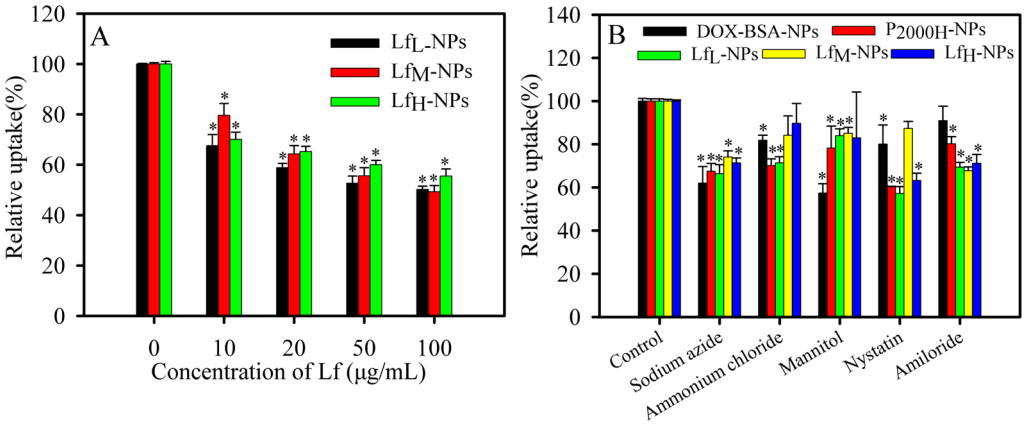

Figure 5. (A) Relative uptake efficiency of Lf-NPs in C6 with preincubation in free Lf (0−100 μg/mL) at 37 °C. (B) Relative uptake efficiency of DOX-BSA-NPs, P_{2000H}-NPs, Lf_L-NPs, Lf_M-NPs, and Lf_H-NPs at 37 °C with various cellular uptake inhibitors in C6. *P < 0.05 compared with control.

molecules on nanocarriers might not achieve high cellular uptake and P_e value. The P_e value of Lf_H-NP was 0.074 cm/h, which was significantly higher (5.69-fold) as compared to that of free DOX. The increase could result from several reasons. First, an appropriate density of ligand on the surface of nanoparticles could enhance the recognition and affinity of Lf receptors, which sequentially triggered Lf-mediated endocytosis and increased accumulation of nanoparticles in cells.[2] Second, the positive zeta potential of Lf on the surface of NPs could promote NPs interacting with the negative cell membrane and uptaking by endocytosis pathways. As shown in Figure 1, when modified with positive Lf, the zeta potential of NPs increased from −13.36 mv for P_{2000H}-NPs to −10.18 mv for Lf_L-NPs, and −9.22 mv for Lf_M-NPs and −8.34 mv for Lf_H-NPs, respectively, suggesting that more Lf_H-NPs would adsorb onto the surface of cells with the help of lower electric repulsion. In addition, the transport of Lf-mediated endocytosis was reported as unidirectional transport,[49] which might improve the uptake of Lf-NPs in the neuron, compared with the conventional NPs. TEER was determined after 24 h incubation period with different samples, and no change was observed (data no shown), suggesting that the increase of permeability was not mediated through damage of tight junctions or permanent changes of membrane function.[29] In the BBB model the competitive inhibition effect was observed when 0.1 mg/mL of free Lf was added and the P_e of Lf_H-NPs decreased to 0.041, confirming that the enhancement of intracellular delivery had high specificity of Lf. The data, along with results from other DOX preparations, supported that Lf_H-NPs had a better permeation enhancement property.

In Vitro Cellular Uptake Assay in BCECs and C6 Cells. In Figure 4A,B, the fluorescent intensities of different preparations in both BCECs and C6 were basically in the following order: Lf_H-NPs ≈ Lf_M-NPs > Lf_L-NPs ≈ DOX-BSA-NPs > P_{2000H}-NPs > DOX solution. The fluorescence intensity of P_{2000H}-NPs was weaker than that of DOX-BSA-NPs in both BCECs and C6. The decreased uptake of P_{2000H}-NPs might be due to the obstacle of hydrophilic PEG to block the endocytosis of nanoparticles into cells.[50] NPs modified with Lf could improve tumor-targeting property significantly. The higher Lf-modified, the stronger the fluorescence intensity, suggesting that the mechanism of uptake of Lf-NPs in C6 could be LRP-mediated endocytosis and reveal Lf concentration dependence.

Competitive inhibition assay was applied to determine whether the endocytosis of Lf-NPs was mediated by Lf receptors. In Figure 5A the data showed that the uptake of Lf-NPs were suppressed by the appearance of free Lf in C6, and less uptake occurred along with the increasing concentration of free Lf, indicating that Lf -mediated endocytosis was one of the pathways for uptaking Lf-NPs in C6. In addition, the bioactivity of Lf was preserved after absorbing to the surface of P_{2000H}-NPs.

To further investigate the endocytosis pathways of unmodified and modified DOX-BSA-NPs in C6 cells, several endocytosis inhibitors were utilized to evaluate the cellular uptake of NPs. In Figure 5B cellular uptake of nanoparticles in the presence of sodium azide, as cell energy metabolism inhibitor, was hindered significantly, suggesting that active transportation was involved in the cellular uptake and was related to energy expenditure. After incubation with ammonium chloride, a cell lysosomotropic agent, the cellular uptake of DOX-BSA-NPs, P_{2000H}-NPs, and Lf_L-NPs decreased significantly, while the influence on Lf_M-NPs and Lf_H-NPs was slight. Ammonium chloride, as a lysosomotropic agent that inhibited the acidification of endosome/lysosome, would lead to a decline in the uptake depending on endosome/lysosome pathway. After incubation with mannitol, inhibitor of clathrin-mediated endocytosis, about 40% of uptake of DOX-BSA-NPs was inhibited, which was markedly higher than that of the other groups (P < 0.05); in addition, we also found that P_{2000H}-NPs, Lf_L-NPs, and Lf_M-NPs were also inhibited by the presence of mannitol. Besides, incubation with NPs in the presence of nystatin was to determine the endocytosis pathways through caveolin-mediated endocytosis in C6 cells.[51] The results indicated that, except for Lf_M-NPs, uptake of other NPs were inhibited by nystatin significantly, suggesting caveolin-mediated endocytosis would not involve in the uptake of Lf_M-NPs. For amiloride, a macropinocytosis inhibitor,[52] except DOX-BSA-NPs, all the other NP groups decrease significantly (P < 0.05).

In Vitro Dual-Targeting Effects. To evaluate the dual-targeting effects, BCECs/C6 coculture model was constructed. In Figure 6, the data showed that the UI of Lf_H-NPs in C6 was 1.5- and 1.8-fold higher than that of DOX-BSA-NPs and P_{2000H}-NPs, respectively. As similar to previous reports, both in vitro uptake and BBB transport experiment exhibited that Lf_H-NPs possessed higher capacity of cellular uptake and penetration of BBB.[53] Moreover, other reports also showed that Lf-modified nanoparticles could prevent active glioma cells from penetrating

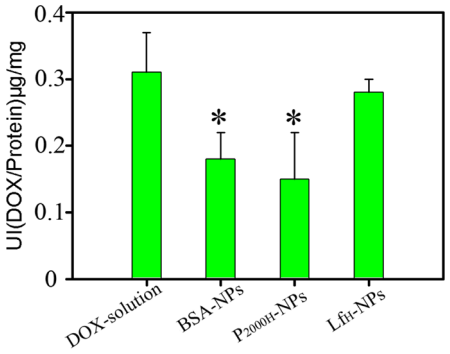

Figure 6. UI of DOX solution, DOX-BSA-NPs, P_{2000H}-NPs, and Lf_H-NPs uptaken by C6 cells in BBB model. Data were presented as the mean ± SD (n = 3). *P < 0.05 compared with DOX solution.

to normal brain parenchyma.[54] Apart from the performance to Lf, the property of nanoparticles also play a role on the BBB passage. Thorne et al. believed that neutral or negatively charged substances up to 64 nm in diameter of quantum dots could passively diffuse through brain tissue and reach neuronal somata.[55] In addition, Zhang et al. reported that chitosan-modified polylactic acid (PLA) nanoparticles with positive zeta potential revealed more stronger BBB penetration than without modified PLA nanoparticles due to the adhesive attraction by electrostatic interaction and bioadhension of chitosan.[56] Thus, in our opinion, zeta potential may play an important role in BBB penetration, but other factors such as particle size and modified materials also affect the BBB passage.

Pharmacokinetics Studies in Rats. The plasma concentration−time curves of DOX after intravenous injection of different preparations in rats are shown in Figure 7. Encapsulation of DOX into BSA-NPs dramatically increased the area under the curve (AUC_{0-1}) and decreased the clearance when compared with DOX solution (P < 0.05). In contrast to DOX-BSA-NPs, P_{2000}-NPs showed higher $t_{1/2}$ and AUC_{0-1} due to modification of mPEG (Table 4). These results demonstrated that the more the mPEG2000 was utilized the thicker SD_{mPEG} and the narrower D_{PEG}. As discussed above, D_{PEG} of P_{2000}-NPs played a crucial role on the absorption of plasma protein on the surface of nanoparticles. Data in Table 1 indicated that P_{2000M}-NPs and P_{2000H}-NPs could hinder most of the plasma protein absorption, which would lead to long circulative effect in vivo. These results were also consistent with the data of in vitro release. Inhibition of the degradation and phagocytosis of RES might be the main reason for prolonged retention of modified BSA-NPs.

However, in the current study, Lf modification seemed to have affected the long-circulation effect of P_{2000H}-NPs. On the one hand, less negative zeta potential would result in long-circulating effect.[41] On the other hand, the hydration of PEG would be interfered with by Lf because of its different hydrophilic and hydrophobic fractions. Another reason is that Lf may cause carrier immunogenicity because of its macromolecule characteristics. Previous studies revealed that recognition by RES might be inhibited by some small specific targeting moieties such as the peptide and antigen-binding fragment (Fab) of antibodies.[57]

In Vivo Tissue Distribution in Glioma Model Rats. Tissue distribution was studied in gliomas of model rats after intravenous injection of DOX solution, DOX-BSA-NPs, P_{2000H}-NPs, and Lf_H-NPs and shown in Figure 8. As anticipated, P_{2000H}-NPs and Lf_H-NPs revealed longer systemic circulation time than DOX solution and DOX-BSA-NPs. In addition, P_{2000H}-NPs and Lf_H-NPs significantly decreased the uptake by liver and spleen when compared with DOX-BSA-NPs. In addition, P_{2000H}-NPs and Lf_H-NPs had also less accumulation of DOX in heart and kidney, which would decrease cardiac and renal toxicity of DOX. As indicated in Figure 7B, P_{2000H}-NPs had longer circulative effect than that of Lf_H-NPs. However, because of the enhancement of uptake and trans-endothelial ability by Lf, Lf_H-NPs in rat brain were significantly increased, especially at 2 h. There were several reasons for the increase of brain targeting of Lf_H-NPs. First, as discussed above, the bioactivity of Lf was preserved in Lf_H-NPs and the specific affinities and binding with Lf receptors on BBB and gliomas cells was not affected by the low endogenous Lf under physiologic conditions.[49] Second, Lf-mediated endocytosis and penetration of BBB was unidirectional, which might increase accumulation of nanoparticles in cells.[58]

■ CONCLUSIONS

A novel dual-targeting brain drug delivery system based on biodegradable BSA-NPs and Lf was designed in the present study. The passive and active targeting property was evaluated by employing different levels of PEG and Lf. PEG-modified BSA-NPs showed improved sustained release and exhibited modification content dependence. In addition, modification with Lf enhanced the sustained release effects. However, no significant difference was observed for different levels of Lf used. Moreover, the MTT result revealed that all of the DOX preparations exhibited high viability for BCEC, but the highest

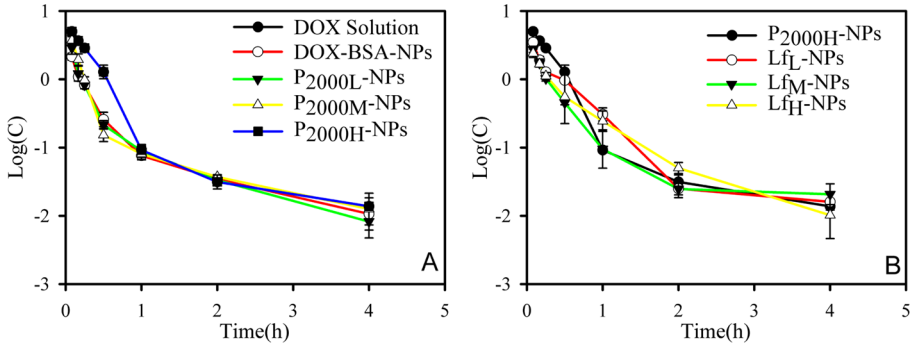

Figure 7. Plasma concentration−time curves of DOX in rats after intravenous administration of (A) DOX solution, DOX-BSA-NPs, P_{2000L}-NPs, P_{2000M}-NPs, and P_{2000H}-NPs and (B) P_{2000H}-NPs, Lf_L-NPs, Lf_M-NPs, and Lf_H-NPs. Data were presented as the mean ± SD (n = 6).

Table 4. Pharmacokinetics Parameters of DOX after Intravenous Administration of DOX Solution and Different DOX-Loaded NPs at a Dose of 5 mg/kg to Rats; Data Were Presented as the Mean ± SD (n = 6)

	parameters					
preparations	C_{max} (mg/L)	$t_{1/2}$ (h)	AUC_{0-1} (mg h/L)	MRT (h)	clearance (L/h)	Vc (L)
DOX-solution	1.37 ± 0.64	0.33 ± 0.12	0.13 ± 0.01	0.20 ± 0.09	16.33 ± 2.05	6.43 ± 1.62
DOX-BSA-NPs	2.15 ± 0.24[a]	0.64 ± 0.02[a]	0.20 ± 0.01[a]	0.25 ± 0.03	7.88 ± 0.29	2.26 ± 0.05[a]
P_{2000L}-NPs	2.94 ± 0.60[a]	0.74 ± 0.14[a]	0.19 ± 0.01[a]	0.25 ± 0.04	6.92 ± 1.33[a]	1.94 ± 0.40[a]
P_{2000M}-NPs	3.75 ± 0.46[a]	0.98 ± 0.13[a]	0.27 ± 0.02[a]	0.30 ± 0.04	5.20 ± 0.74[a]	1.27 ± 0.30[a]
P_{2000H}-NPs	5.01 ± 0.33[a]	1.86 ± 0.14[a]	0.39 ± 0.06[a]	0.42 ± 0.05[a]	2.70 ± 0.20[a]	0.62 ± 0.05[a]
Lf_L-NPs	3.49 ± 0.42[a]	1.41 ± 0.09[a]	0.29 ± 0.03[a]	0.39 ± 0.04[a]	3.54 ± 0.22[a]	1.50 ± 0.18[a]
Lf_M-NPs	2.75 ± 0.29[a]	0.88 ± 0.05[a]	0.20 ± 0.04[a]	0.27 ± 0.04	5.66 ± 0.31[a]	1.63 ± 0.24[a]
Lf_H-NPs	2.42 ± 0.34[a]	1.07 ± 0.19[a]	0.30 ± 0.07[a]	0.40 ± 0.14[a]	4.80 ± 0.94[a]	2.01 ± 0.15[a]

[a]*P < 0.05, versus DOX-solution.

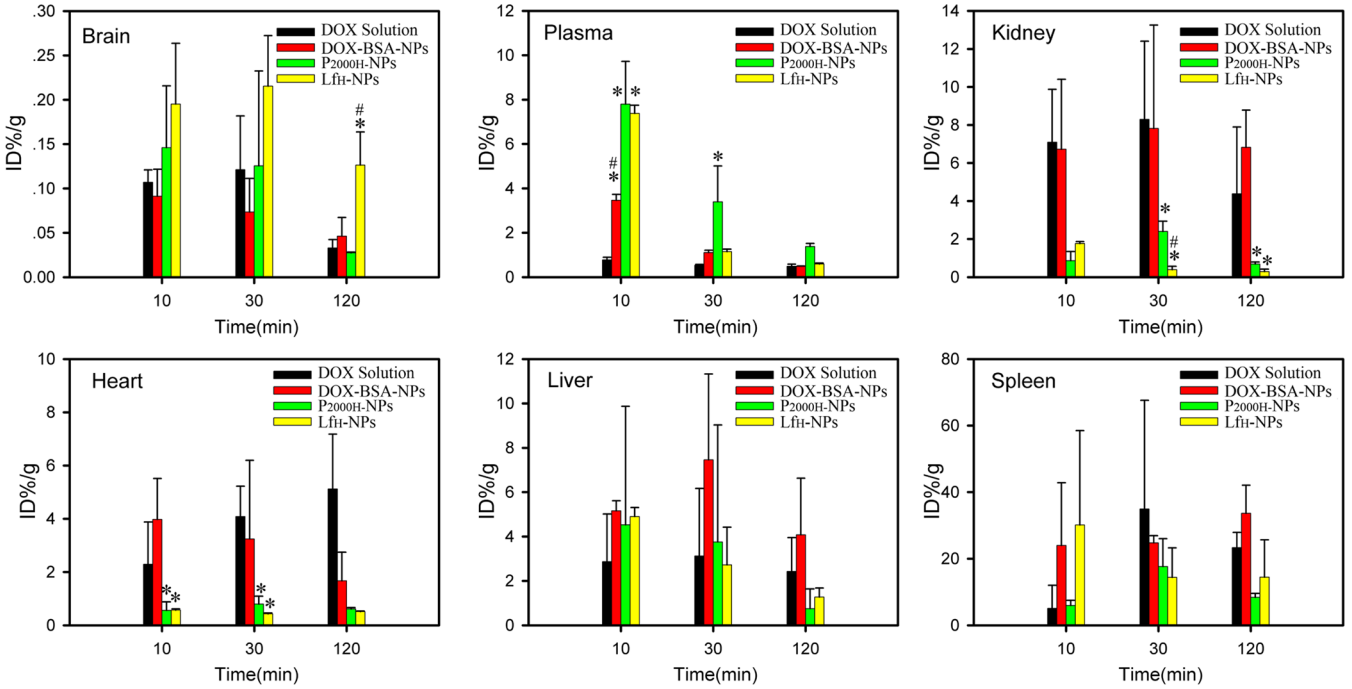

Figure 8. Tissue distribution of DOX after intravenous administration of DOX solution, DOX-BSA-NPs, P_{2000H}-NPs, and Lf_H-NPs in glioma model rats. Data were presented as the mean ± SD (n = 3). *P < 0.05 compared with DOX solution; #P < 0.05 compared with P_{2000H}-NPs.

cytotoxicity was found for high level modifications of Lf. Because of the ability of recognition of Tf receptors, Lf_H-NPs had a better permeation enhancement property, increased dual-targeting effect for brain delivery of nanoparticles and facilitated the uptake of DOX in the brain tissue. Therefore, as a potential dual-targeting drug delivery system, Lf-NPs would be utilized for targeting therapy of brain gliomas.

AUTHOR INFORMATION

Corresponding Author

*(Y.Xi.) Tel/Fax: +86 25 83271079. E-mail: cpuyanyuxiao@163.com.

Author Contributions

†Z.S., L.X., and Y.C. contributed equally to this work.

Notes

The authors declare no competing financial interest.

ACKNOWLEDGMENTS

This work was supported by the Natural Science Foundation of Jiangsu Province (Program No. BK20130655), College Students Innovation Project for the R&D of Novel Drugs (Program No. J1030830), and the National College Students' innovation entrepreneurial training program (Program No. G12097).

REFERENCES

(1) Fernandez, A. P.; Serrano, J.; Amorim, M. A.; Pozo-Rodrigalvarez, A.; Martinez-Murillo, R. Adrenomedullin and nitric oxide: implications for the etiology and treatment of primary brain tumors. *CNS Neurol. Disord. Drug Targets* **2011**, *10* (7), 820−33.

(2) Pang, Z.; Feng, L.; Hua, R.; Chen, J.; Gao, H.; Pan, S.; Jiang, X.; Zhang, P. Lactoferrin-conjugated biodegradable polymersome holding doxorubicin and tetrandrine for chemotherapy of glioma rats. *Mol. Pharmaceutics* **2010**, *7* (6), 1995−2005.

(3) Taylor, T. E.; Furnari, F. B.; Cavenee, W. K. Targeting EGFR for treatment of glioblastoma: molecular basis to overcome resistance. *Curr. Cancer Drug Targets* **2012**, *12* (3), 197−209.

(4) Li, Y.; He, H.; Jia, X.; Lu, W. L.; Lou, J.; Wei, Y. A dual-targeting nanocarrier based on poly(amidoamine) dendrimers conjugated with transferrin and tamoxifen for treating brain gliomas. *Biomaterials* **2012**, *33* (15), 3899−3908.

(5) Ying, X.; Wen, H.; Lu, W. L.; Du, J.; Guo, J.; Tian, W.; Men, Y.; Zhang, Y.; Li, R. J.; Yang, T. Y.; Shang, D. W.; Lou, J. N.; Zhang, L. R.; Zhang, Q. Dual-targeting daunorubicin liposomes improve the therapeutic efficacy of brain glioma in animals. *J. Controlled Release* **2010**, *141* (2), 183−92.
(6) He, H.; Li, Y.; Jia, X. R.; Du, J.; Ying, X.; Lu, W. L.; Lou, J. N.; Wei, Y. PEGylated poly(amidoamine) dendrimer-based dual-targeting carrier for treating brain tumors. *Biomaterials* **2011**, *32* (2), 478−87.
(7) Salvati, A.; Pitek, A. S.; Monopoli, M. P.; Prapainop, K.; Bombelli, F. B.; Hristov, D. R.; Kelly, P. M.; Aberg, C.; Mahon, E.; Dawson, K. A. Transferrin-functionalized nanoparticles lose their targeting capabilities when a biomolecule corona adsorbs on the surface. *Nat. Nanotechnol.* **2012**, *8* (2), 137−43.
(8) Fillebeen, C.; Ruchoux, M. M.; Mitchell, V.; Vincent, S.; Benaïssa, M. Lactoferrin is synthesized by activated microglia in the human substantia nigra and its synthesis by the human microglial CHME cell line is upregulated by tumor necrosis factor alpha or 1-methyl-4-phenylpyridinium treatment. *Brain Res. Mol. Brain Res.* **2001**, *96*, 103−113.
(9) Pang, Z.; Gao, H.; Yu, Y.; Guo, L.; Chen, J.; Pan, S.; Ren, J.; Wen, Z.; Jiang, X. Enhanced intracellular delivery and chemotherapy for glioma rats by transferrin-conjugated biodegradable polymersomes loaded with doxorubicin. *Bioconjugate Chem.* **2011**, *22* (6), 1171−80.
(10) Jeffrey, P. D.; Bewley, M. C.; Macgillivray, R. T.; Mason, A. B.; Woodworth, R. C.; Baker, E. N. Ligand-induced conformational change in transferrins: crystal structure of the open form of the N-terminal half-molecule of human transferrin. *Biochemistry* **1998**, *37* (40), 13978−86.
(11) Suzuki, Y. A.; Lopez, V.; Lonnerdal, B. Mammalian lactoferrin receptors: structure and function. *Cell. Mol. Life Sci.* **2005**, *62* (22), 2560−75.
(12) Dashper, S. G.; Pan, Y.; Veith, P. D.; Chen, Y. Y.; Toh, E. C.; Liu, S. W.; Cross, K. J.; Reynolds, E. C. Lactoferrin inhibits *Porphyromonas gingivalis* proteinases and has sustained biofilm inhibitory activity. *Antimicrob. Agents Chemother.* **2012**, *56* (3), 1548−56.
(13) Mohsen, J.; Zahra, B. Protein nanoparticle: A unique system as drug delivery vehicles. *Afr. J. Biotechnol.* **2008**, *7* (25), 4926−4934.
(14) Kumar, M. N. V. R. Nano and microparticles as controlled drug delivery devices. *J. Pharm. Pharm. Sci.* **2000**, *3* (2), 234−258.
(15) Rahimnejad, M.; Mokhtarian, N.; Ghasemi, M. Production of protein nanoparticles for food and drug delivery system. *Afr. J. Biotechnol.* **2009**, *8* (19), 4738−4743.
(16) Kouchakzadeh, H.; Shojaosadati, S. A.; Maghsoudi, A.; Vasheghani Farahani, E. Optimization of PEGylation conditions for BSA nanoparticles using response surface methodology. *AAPS PharmSciTech.* **2010**, *11* (3), 1206−11.
(17) Shen, J.; Wang, Y.; Ping, Q.; Xiao, Y.; Huang, X. Mucoadhesive effect of thiolated PEG stearate and its modified NLC for ocular drug delivery. *J. Controlled Release* **2009**, *137* (3), 217−23.
(18) Sun, M.; Wang, Y.; Shen, J.; Xiao, Y.; Su, Z.; Ping, Q. Octreotide-modification enhances the delivery and targeting of doxorubicin-loaded liposomes to somatostatin receptors expressing tumor in vitro and in vivo. *Nanotechnology* **2010**, *21* (47), 475101.
(19) Mao, S. J.; Hou, S. X.; Zhang, L. K.; Jin, H.; Bi, Y. Q.; Jiang, B. Preparation of bovine serum albumin nanoparticles surface-modified with glycyrrhizin. *Yao Xue Xue Bao.* **2003**, *38* (10), 787−90.
(20) Dreis, S.; Rothweiler, F.; Michaelis, M.; Cinatl, J., Jr.; Kreuter, J.; Langer, K. Preparation, characterisation and maintenance of drug efficacy of doxorubicin-loaded human serum albumin (HSA) nanoparticles. *Int. J. Pharm.* **2007**, *341* (1−2), 207−14.
(21) Chen, Y. N.; Xiao, Y. Y.; Su, Z. G.; Ping, Q. N.; Zhang, C. Effect of preparation process of doxorubicin albumin nanoparticles on physicochemical properties, in vitro release and pharmacokinetics. *Chin. J. Pharm.* **2012**, *43* (6), 432−437.
(22) Peracchia, M. T.; Vauthier, C.; Passirani, C.; Couvreur, P.; Labarre, D. Complement consumption by poly(ethylene glycol) in different conformations chemically coupled to poly(isobutyl 2-cyanoacrylate) nanoparticles. *Life Sci.* **1997**, *61* (7), 749−61.
(23) Weber, C.; Coester, C.; Kreuter, J.; Langer, K. Desolvation process and surface characterisation of protein nanoparticles. *Int. J. Pharm.* **2000**, *194* (1), 91−102.
(24) Ko, S.; Gunasekaran, S. Preparation of sub-100-nm beta-lactoglobulin (BLG) nanoparticles. *J. Microencapsul.* **2006**, *23* (8), 887−98.
(25) Deracinois, B.; Duban-Deweer, S.; Pottiez, G.; Cecchelli, R.; Karamanos, Y.; Flahaut, C. TNAP and EHD1 are over-expressed in bovine brain capillary endothelial cells after the re-induction of blood-brain barrier properties. *PLoS One* **2012**, *7* (10), e48428.
(26) Ke, W. L.; Shao, K.; Huang, R. Q.; Han, L.; Liu, Y.; Li, J. F.; Kuang, Y. Y.; Ye, L. Y.; Lou, J. N.; Jiang, C. Gene delivery targeted to the brain using an Angiopep-conjugated polyethyleneglycol-modified polyamidoamine dendrimer. *Biomaterials* **2009**, *30* (36), 6976−6985.
(27) Xie, Y.; Ye, L. Y.; Zhang, X. B.; Hou, X. P.; Lou, J. N. Establishment of an in vitro model of brain-blood barrier. *Beijing Da Xue Xue Bao.* **2004**, *36* (4), 435−438.
(28) He, H.; Li, Y.; Jia, X. R.; Du, J.; Ying, X.; Lu, W. L.; Lou, J. N.; Wei, Y. PEGylated Poly(amidoamine) dendrimer-based dual-targeting carrier for treating brain tumors. *Biomaterials.* **2011**, *32* (2), 478−487.
(29) Makhlof, A.; Werle, M.; Tozuka, Y.; Takeuchi, H. A mucoadhesive nanoparticulate system for the simultaneous delivery of macromolecules and permeation enhancers to the intestinal mucosa. *J. Controlled Release* **2011**, *149* (1), 81−88.
(30) Su, Z.; Shi, Y.; Xiao, Y.; Sun, M.; Ping, Q.; Zong, L.; Li, S.; Niu, J.; Huang, A.; You, W.; Chen, Y.; Chen, X.; Fei, J.; Tian, J. Effect of octreotide surface density on receptor-mediated endocytosis in vitro and anticancer efficacy of modified nanocarrier in vivo after optimization. *Int. J. Pharm.* **2013**, *447* (1−2), 281−92.
(31) Qian, Z.; Dominguez, S. R.; Holmes, K. V. Role of the spike glycoprotein of human Middle East respiratory syndrome coronavirus (MERS-CoV) in virus entry and syncytia formation. *PLoS One* **2013**, *8* (10), e76469.
(32) Perry, J. W.; Wobus, C. E. Endocytosis of murine norovirus 1 into murine macrophages is dependent on dynamin II and cholesterol. *J. Virol.* **2010**, *84* (12), 6163−76.
(33) Durymanov, M. O.; Beletkaia, E. A.; Ulasov, A. V.; Khramtsov, Y. V.; Trusov, G. A.; Rodichenko, N. S.; Slastnikova, T. A.; Vinogradova, T. V.; Uspenskaya, N. Y.; Kopantsev, E. P.; Rosenkranz, A. A.; Sverdlov, E. D.; Sobolev, A. S. Subcellular trafficking and transfection efficacy of polyethylenimine-polyethylene glycol polyplex nanoparticles with a ligand to melanocortin receptor-1. *J. Controlled Release* **2012**, *163* (2), 211−9.
(34) Koivusalo, M.; Welch, C.; Hayashi, H.; Scott, C. C.; Kim, M.; Alexander, T.; Touret, N.; Hahn, K. M.; Grinstein, S. Amiloride inhibits macropinocytosis by lowering submembranous pH and preventing Rac1 and Cdc42 signaling. *J. Cell Biol.* **2010**, *188* (4), 547−63.
(35) Zu, Y.; Zhang, Y.; Zhao, X.; Zhang, Q.; Liu, Y.; Jiang, R. Optimization of the preparation process of vinblastine sulfate (VBLS)-loaded folate-conjugated bovine serum albumin (BSA) nanoparticles for tumor-targeted drug delivery using response surface methodology (RSM). *Int. J. Nanomed.* **2009**, *4*, 321−33.
(36) Shimada, K.; Miyagishima, A.; Sadzuka, Y.; Nozawa, Y.; Mochizuki, Y.; Ohshima, H.; Hirota, S. Determination of the thickness of the fixed aqueous layer around polyethyleneglycol-coated liposomes. *J. Drug Targeting* **1995**, *3* (4), 283−9.
(37) Fang, C.; Shi, B.; Pei, Y. Y.; Hong, M. H.; Wu, J.; Chen, H. Z. In vivo tumor targeting of tumor necrosis factor-alpha-loaded stealth nanoparticles: effect of MePEG molecular weight and particle size. *Eur. J. Pharm. Sci.* **2006**, *27* (1), 27−36.
(38) Utreja, S.; Khopade, A. J.; Jain, N. K. Lipoprotein-mimicking biovectorized systems for methotrexate delivery. *Pharm. Acta Helv.* **1999**, *73* (6), 275−9.
(39) Fede, C.; Selvestrel, F.; Compagnin, C.; Mognato, M.; Mancin, F.; Reddi, E.; Celotti, L. The toxicity outcome of silica nanoparticles (Ludox(R)) is influenced by testing techniques and treatment modalities. *Anal. Bioanal. Chem.* **2012**, *404* (6−7), 1789−802.

(40) Soong, R.; Macdonald, P. M. PEG molecular weight and lateral diffusion of PEG-ylated lipids in magnetically aligned bicelles. *Biochim. Biophys. Acta* **2007**, *1768* (7), 1805−14.
(41) Gref, R.; Domb, A.; Quellec, P.; Blunk, T.; Muller, R. H.; Verbavatz, J. M.; Langer, R. The controlled intravenous delivery of drugs using Peg-coated sterically stabilized nanospheres. *Adv. Drug Delivery Rev.* **1995**, *16* (23), 215−233.
(42) Avraham, H. K.; Lee, T. H.; Koh, Y.; Kim, T. A.; Jiang, S.; Sussman, M.; Samarel, A. M.; Avraham, S. Vascular endothelial growth factor regulates focal adhesion assembly in human brain microvascular endothelial cells through activation of the focal adhesion kinase and related adhesion focal tyrosine kinase. *J. Biol. Chem.* **2003**, *278* (38), 36661−8.
(43) Barzegar-Jalali, M.; Adibkia, K.; Valizadeh, H.; Shadbad, M. R.; Nokhodchi, A.; Omidi, Y.; Mohammadi, G.; Nezhadi, S. H.; Hasan, M. Kinetic analysis of drug release from nanoparticles. *J. Pharm. Pharm. Sci.* **2008**, *11* (1), 167−77.
(44) Morales, M. E.; Gallardo Lara, V.; Calpena, A. C.; Domenech, J.; Ruiz, M. A. Comparative study of morphine diffusion from sustained release polymeric suspensions. *J. Controlled Release* **2004**, *95* (1), 75−81.
(45) Su, Z.; Niu, J.; Xiao, Y.; Ping, Q.; Sun, M.; Huang, A.; You, W.; Sang, X.; Yuan, D. Effect of octreotide-polyethylene glycol(100) monostearate modification on the pharmacokinetics and cellular uptake of nanostructured lipid carrier loaded with hydroxycamptothecine. *Mol. Pharmaceutics* **2011**, *8* (5), 1641−1651.
(46) Steiniger, S. C.; Kreuter, J.; Khalansky, A. S.; Skidan, I. N.; Bobruskin, A. I.; Smirnova, Z. S.; Severin, S. E.; Uhl, R.; Kock, M.; Geiger, K. D.; Gelperina, S. E. Chemotherapy of glioblastoma in rats using doxorubicin-loaded nanoparticles. *Int. J. Cancer.* **2004**, *109* (5), 759−67.
(47) Su, Z.; Niu, J.; Xiao, Y.; Ping, Q.; Sun, M.; Huang, A.; You, W.; Sang, X.; Yuan, D. Effect of octreotide-polyethylene glycol(100) monostearate modification on the pharmacokinetics and cellular uptake of nanostructured lipid carrier loaded with hydroxycamptothecine. *Mol. Pharmaceutics* **2011**, *8* (5), 1641−51.
(48) Wan, F.; You, J.; Sun, Y.; Zhang, X. G.; Cui, F. D.; Du, Y. Z.; Yuan, H.; Hu, F. Q. Studies on PEG-modified SLNs loading vinorelbine bitartrate (I): preparation and evaluation in vitro. *Int. J. Pharm.* **2008**, *359* (1−2), 104−10.
(49) Talukder, M. J.; Takeuchi, T.; Harada, E. Receptor-mediated transport of lactoferrin into the cerebrospinal fluid via plasma in young calves. *J. Vet. Med. Sci.* **2003**, *65* (9), 957−64.
(50) Hu, Y.; Xie, J.; Tong, Y. W.; Wang, C. H. Effect of PEG conformation and particle size on the cellular uptake efficiency of nanoparticles with the HepG2 cells. *J. Controlled Release* **2007**, *118* (1), 7−17.
(51) Mo, R.; Jin, X.; Li, N.; Ju, C.; Sun, M.; Zhang, C.; Ping, Q. The mechanism of enhancement on oral absorption of paclitaxel by *N*-octyl-*O*-sulfate chitosan micelles. *Biomaterials* **2011**, *32* (20), 4609−20.
(52) Jones, A. T. Macropinocytosis: searching for an endocytic identity and role in the uptake of cell penetrating peptides. *J. Cell Mol. Med.* **2007**, *11* (4), 670−84.
(53) Yu, Y.; Pang, Z.; Lu, W.; Yin, Q.; Gao, H.; Jiang, X. Self-assembled polymersomes conjugated with lactoferrin as novel drug carrier for brain delivery. *Pharm. Res.* **2012**, *29* (1), 83−96.
(54) Misra, A.; Ganesh, S.; Shahiwala, A.; Shah, S. P. Drug delivery to the central nervous system: a review. *J. Pharm. Pharm. Sci.* **2003**, *6* (2), 252−73.
(55) Thorne, R. G.; Nicholson, C. In vivo diffusion analysis with quantum dots and dextrans predicts the width of brain extracellular space. *Proc. Natl. Acad. Sci. U.S.A.* **2006**, *103* (14), 5567−72.
(56) Zhang, X.; Liu, L.; Chai, G.; Li, F. Brain pharmacokinetics of neurotoxin-loaded PLA nanoparticles modified with chitosan after intranasal administration in awake rats. *Drug Dev. Ind. Pharm.* **2013**, *39* (11), 1618−24.
(57) Maruyama, K.; Takahashi, N.; Tagawa, T.; Nagaike, K.; Iwatsuru, M. Immunoliposomes bearing polyethyleneglycol-coupled Fab' fragment show prolonged circulation time and high extravasation into targeted solid tumors in vivo. *FEBS Lett.* **1997**, *413* (1), 177−80.
(58) Fillebeen, C.; Descamps, L.; Dehouck, M. P.; Fenart, L.; Benaissa, M.; Spik, G.; Cecchelli, R.; Pierce, A. Receptor-mediated transcytosis of lactoferrin through the blood−brain barrier. *J. Biol. Chem.* **1999**, *274* (11), 7011−7.